

Supporting Information

Carbon and nutrient mobilization across inundation gradients in an
emerging freshwater delta

Matthew J. Berens,^{1,*,+} Geoff Schwaner,¹ and Elizabeth M. Herndon¹

¹Environmental Sciences Division, Oak Ridge National Laboratory, Oak Ridge, TN 37831

⁺Current address: North Carolina Department of Agriculture and Consumer Services, Raleigh, NC 27699

*corresponding author: matthew.berens@ncagr.gov

5 Pages, 1 Figure, 3 Tables

S1 Experimental Section

S1.1 Site Description

In the main text, we define the Old Transect (OT) and Young Transect (YT) with respect to the time since subaerial emergence of the region on Mike Island where the samples were collected (Figure S1a). We use island age rather than developmental and/or weathering history of the soils when describing the study transects for consistency with previous studies. The island first became subaerial in 1973 and has been steadily building land since.¹ In general, sediment deposition from the Atchafalaya River via the Wax Lake Outlet is causing the downstream progression of delta aggradation such that regions on the proximal end of the island became subaerial earlier than regions closer to the distal end of the island. For our study sites, the time since subaerial emergence was estimated from Twilley et al. (2018), who initially derived depositional history using a model adapted from Wellner et al. (2005) and additional satellite imagery. From these data, we estimated the subaerial exposure dates of the OT and YT as shown in Figure S1c.

To further quantify the growth of land at our study sites, we estimated sedimentation rates using data collected by the Delta-X campaign from nearby locations. Delta-X performed biannual feldspar sediment accretion measurements from 2019-2023 from supratidal and subtidal zones of an older region of the island (WLD_T1) near our OT study site, and intertidal and subtidal zones of a younger region of the island (WLD_T3) near our YT site (Figure S1a). These data show that intertidal and supratidal zones have the highest and lowest sedimentation rates, respectively, while subtidal zones have intermediate values that were similar across transects (Figure S1b-c). Furthermore, these data show that the subtidal zones of each transect are accreting at similar rates, which provides further evidence that the OT region of Mike Island, which became subaerial before the YT, is indeed older than the YT study transect.

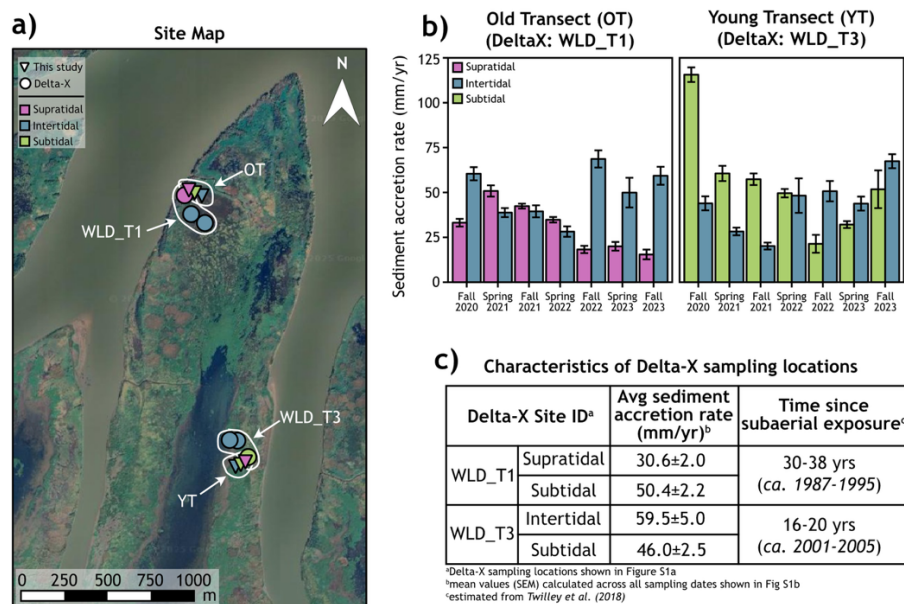


Figure S1. (a) Site map of Mike Island showing the location of Old Transect (OT) and Young Transect (YT) study sites in relation to the field sites used for sediment accretion measurements in the Delta-X campaign. (b) Average sediment accretion rates measured by the Delta-X campaign. All error bars represent the standard deviation of triplicate measurements at triplicate plots (N=9 total). (c) Summary of average sediment accretion rates and time since subaerial emergence for Delta-X sites. Accretion rates represent the average across all time points for a given site.

S1.2 Mesocosm incubation and sampling

The chemical composition of surface water at each study site was evaluated at the time of soil collection. The results, shown in Table S1, were used as the basis for the composition of the water used during the incubation experiment.

Table S1. Chemical composition of surface water at Wax Lake Delta field sites during soil collection.

Transect^a	E_h^b (mV)	SpC^c (μS/cm)	pH	DOC (μmol/L)	DIC (μmol/L)	Ca (μmol/L)	Cl⁻ (μmol/L)	Total Fe (μmol/L)	Mg (μmol/L)	Na (μmol/L)	P (μmol/L)	SO₄²⁻ (μmol/L)
Young Transect (YT)	+212	232	7.67	568	1789	925	451	1.2	397	704	<16 ^d	175
Old Transect (OT)	+178	362	7.44	1077	2198	995	428	51	455	1080	19	11

^aYT was sampled March 8, 2025; OT was sampled March 9, 2025.
^bConverted from measured ORP (mV vs Ag/AgCl) to Eh (mV vs SHE) by adding 209 mV.
^cSpC = Specific conductance.
^dBelow instrument detection limit of 16 μmol/L.

S2 Additional Results

Table S2. Measured carbon dioxide (CO₂) fluxes during soil incubations normalized to soil dry mass (mmol CO₂·kg⁻¹·d⁻¹) and mesocosm surface area (mmol CO₂·m⁻²·d⁻¹). These data correspond to the results presented in Figures 3 and 4 in the main text.

Site	Transect	Cumulative release	Rate (0-21 d)		Rate (22-30 d)	
		(mmol CO ₂ ·kg ⁻¹)	(mmol CO ₂ ·kg ⁻¹ ·d ⁻¹)	(mmol CO ₂ ·m ⁻² ·d ⁻¹)	(mmol CO ₂ ·kg ⁻¹ ·d ⁻¹)	(mmol CO ₂ ·m ⁻² ·d ⁻¹)
Supratidal	OT	19.1 ± 0.2	0.92 ± 0.31	47.2 ± 16.0	0.132 ± 0.001	6.8 ± 0.1
	YT	8.0 ± 1.4	0.39 ± 0.02	25.1 ± 1.6	0.059 ± 0.003	3.8 ± 0.2
Intertidal	OT	29.6 ± 2.0	1.36 ± 0.02	40.9 ± 0.6	0.803 ± 0.016	24.1 ± 0.5
	YT	6.4 ± 1.1	0.30 ± 0.01	16.2 ± 0.6	0.154 ± 0.009	8.4 ± 0.5
Subtidal	OT	3.7 ± 1.1	0.18 ± 0.02	8.5 ± 1.0	0.198 ± 0.004	9.4 ± 0.2
	YT	2.6 ± 0.8	0.13 ± 0.01	8.2 ± 0.8	0.162 ± 0.001	10.3 ± 0.1

Table S3. Average solute releases (mean±standard deviation) during inundated periods of intertidal experiments normalized to total soil mass ($\text{mmol}\cdot\text{kg}^{-1}$)^a and DOC normalized to total soil C in the mesocosm soil ($\text{mmol}\cdot\text{mol C}^{-1}$)^b.

	DOC ($\text{mmol}\cdot\text{kg}^{-1}$)	DOC ($\text{mmol}\cdot\text{mol C}^{-1}$)	Fe ($\text{mmol}\cdot\text{kg}^{-1}$)	P ($\text{mmol}\cdot\text{kg}^{-1}$)	Ca ($\text{mmol}\cdot\text{kg}^{-1}$)	Mg ($\text{mmol}\cdot\text{kg}^{-1}$)
<i>Old Transect (OT)</i>						
Intertidal 1	37.8±4.4	9.3±6.0	8.3±1.1	0.56±0.06	22.1±8.2	13.1±9.0
Intertidal 2	28.0±4.3	6.9±1.1	4.3±0.7	0.31±0.05	13.7±5.5	8.1±3.1
Intertidal 3	23.9±1.0	5.9±0.3	1.0±0.2	0.21±0.03	4.4±3.6	2.4±1.9
Intertidal 4	3.5±0.1	0.9±0.1	0.8±0.1	0.02±0.01	2.0±0.5	0.9±0.3
Total intertidal	93.2±6.3	23.0±6.1	14.8±1.3	1.09±0.08	42.3±10.5	24.5±9.7
Subtidal	16.4±0.1	9.4±0.2	4.1±0.1	0.85±0.04	21.7±0.2	10.2±0.1
<i>Young Transect (YT)</i>						
Intertidal 1	23.9±2.2	14.0±1.3	2.0±0.6	0.25±0.03	16.1±4.1	12.1±4.5
Intertidal 2	11.6±3.0	6.8±1.8	1.1±0.5	0.22±0.04	8.0±3.8	4.5±2.1
Intertidal 3	5.9±0.7	3.5±0.4	0.4±0.1	0.12±0.02	3.2±2.5	1.6±1.3
Intertidal 4	1.6±0.1	1.0±0.1	0.2±0.1	0.05±0.01	3.0±0.3	1.5±0.2
Total intertidal	43.0±3.8	25.2±2.2	3.7±0.7	0.64±0.05	30.3±6.1	19.8±5.2
Subtidal	22.9±0.4	10.8±0.1	5.3±0.1	1.46±0.06	27.2±0.5	13.5±6.5